Indian Journal of Chemistry
Vol. 60A, April 2021, pp. 519-530

The potential anticancer activities of platinum(II) complexes with tridentate N'N'N' pincer ligands

Jamal Lasri[a,*], Magda M Aly[b,f], Naser E Eltayeb[a], Mona A Alamri[c,d], Bandar A Babgi[c] & Mostafa A Hussien[c,e]

[a]Department of Chemistry, Rabigh College of Science and Arts, King Abdulaziz University, Jeddah, Saudi Arabia
[b]Department of Biology, Faculty of Science, King Abdulaziz University, Jeddah 21589, Saudi Arabia
[c]Department of Chemistry, Faculty of Science, King Abdulaziz University, Jeddah 21589, Saudi Arabia
[d]Department of Chemistry, College of Science and Arts, Qassim University, Buraydah 51452, Saudi Arabia
[e]Department of Chemistry, Faculty of Science, Port Said University, Port Said 42521, Egypt
[f]Botany and Microbiology Department, Faculty of Science, Kafrelsheikh University, Egypt

*E-mail: jlasri@kau.edu.sa

Received; 08 April 2020; revised and accepted 29 January 2021

Treatment of *cis/trans*-[$PtCl_2(N{\equiv}CR)_2$] **1** (R = CH_3 (**1a**), C_2H_5 (**1b**), C_6H_5 (**1c**), $CH_2C_6H_4$(*p*-CH_3) (**1d**)) with 1,3-diiminoisoindoline **2** gives access to the corresponding symmetrical (1,3,5,7,9-pentaazanona-1,3,6,8-tetraenato) platinum(II) complexes [PtCl{NH=C(R)N=C(C_6H_4)NC=NC(R)=NH}] **3a-d**, in good yields (65–77%). The compounds **3a-d** have been characterized by IR, ^{1}H, ^{13}C and DEPT-135 NMR spectroscopies, ESI-MS and elemental analyses. GIAO/DFT studies have been performed to confirm the molecular structure of the platinum(II)-pincer **3d** by comparing the experimental and theoretical ^{1}H and ^{13}C NMR chemical shifts, and it has shown good correlations between experimental and calculated chemical shifts for proton and carbon with correlation coefficients of 0.9947 and 0.9968, respectively. Molecular electrostatic potential is used to investigate the nucleophilic or electrophilic regions in the molecule **3d**. The antimicrobial activities of compounds **3a-d** are determined against different bacterial pathogens and yeasts. No toxicity is recorded against *Artemia saline* as a test organism for **3a-c**, while moderate toxicity is found for **3d** at 0.62 µM. Comparable antitumor activities are found for **3a-d** against human colon HCT116 and human breast (MCF-7) cancer cell lines. The complexes **3a-d** have shown good binding affinities to ct-DNA in the range of $6.00{\times}10^5$ to $8.33{\times}10^5$ and the conducted molecular docking studies suggest an intercalation mode of binding with DNA by the isoindole fragment of the ligands. Overall, this class of tridentate ligands have shown good potential in designing platinum(II) complexes with promising biological and anticancer activities. Moreover, the presence of the side chains on the ligands provides great design flexibility by introducing some chemical and/or physical characteristics.

Keywords: Platinum(II) complexes, Pincer ligands, Antimicrobial, Anticancer, DNA-binding, Molecular docking

Cisplatin has gained clinical approval in 1978 as a drug in treating some types of cancer and around 50% of the chemotherapeutic protocols include cisplatin[1]. However, its severe side effects motivated researchers to design alternatives with enhanced features through several approaches including the alteration of the coordination sphere around the platinum-metal centre. Carboplatin (clinically approved in 1986) and oxaliplatin (clinically approved in 1996) were introduced as alternatives with less side effects with comparable effectiveness against some cancer cell lines but with some problems involving the solubility and delivery[2]. Recently, there is an increasing interest in the preparation of platinum(II) compounds bearing bidentate *N*-donor ligands as drugs; these compounds display good bioactivity combined with low toxicity. Research has been paying attention to pyridine-based platinum(II) compounds due to their similar or better cytotoxicity compared to cisplatin against some cancer cell lines[3]. Planar ligands are advantageous as their metal-complexes have low tendencies towards thiol deactivation[4]. Remarkable anticancer activities were highlighted for a range of platinum(II) compounds functionalized with pyridyl Schiff bases and their mechanism of action was induced by apoptosis[5]. Platinum(II) compounds containing amino pyridine derivatives showed an intercalation mode of binding with DNA with excellent cytotoxicity compared to cisplatin when tested against three different tumor cell lines[6]. Cytotoxicity against breast, lung and human cervical cancer cell lines was reported for a range of platinum(II) compounds with amino pyridine ligands and found to be better than that reported for cisplatin[6b]. Imino-quinolyl containing

platinum(II) complexes were assessed for their anticancer properties *in vitro* and found to be cytotoxic against human colon (HT-29) and human breast (MCF-7) cancer cell lines[7]. Tridentate ligands have been employed recently in designing anticancer platinum complexes. In the past few years, many platinum complexes bearing π-conjugated polypyridyl ligands have been under enormous interest due to their anticancer activities[8]. This interest stems from the ability of the planar aromatic ligands to interact noncovalently, specifically the intercalation mode of binding between base pairs in the DNA. Lippard et al. reported the first X-ray structure of intercalating [Pt(terpy)(S-CH_2CH_2-OH)] between adjacent DNA base pairs, causing the unwinding of the DNA[9]. More complexes with other leaving groups bind covalently to the guanine bases similar to cisplatin[10]. In addition, several platinum(II) terpyridine complexes with different functionalized thiol ligands have been synthesized and found to be active against the murine leukemia cell line (L1210)[11]. Despite the parent complex with labile chloro which found to be ineffective, other variations to groups attached to platinum such as picoline and acetylides have better anticancer activities[12]. Groove binding and highly active anticancer agent was obtained when the terpyridine ligand was decorated with tert-butyl group[13] (Fig. 1).

Herein, we are examining for the first time our neutral platinum(II) complexes with isoindole-containing tridentate ligands[14] as DNA-intercalating agents and evaluating their antimicrobial, toxicity and antitumor activities. The tridentate ligands have the isoindole planar fragment with two side alkyl or aryl side chains; the alkyl and aryl arms can be utilized to tune the dimensions of the complexes, in addition to their contributions in some physical (*e.g.,* hydrophilicity, hydrophobicity, etc.) and chemical (*e.g.,* noncovalent interactions) properties.

Materials and Methods

Instrumentations

^{1}H, ^{13}C and DEPT-135 NMR spectra (in $CDCl_3$) were measured on a Bruker Avance III HD 600 MHz (Ascend™ Magnet) spectrometer at ambient temperature. ^{1}H, ^{13}C and DEPT-135 chemical shifts (δ) are expressed in ppm relative to trimethylsilane (TMS). Infrared spectra (IR) were recorded on an Alpha Bruker FT-IR instrument in KBr pellets. High resolution electrospray ionization mass spectrometry (ESI-MS) spectra were recorded using impact II™ mass spectrometer from Bruker; the mass spectrometry is reported as *m/z*. In our previously work, the synthesis of (1,3,5,7,9-Pentaazanona-1,3,6,8-tetraenato) platinum(II) complexes [PtCl{NH=C(R)N=C(C_6H_4)NC=NC(R)=NH}] (R = CH_3 (**3a**), C_2H_5 (**3b**), C_6H_5 (**3c**)) was described[14].

Preparation of the nitrile platinum(II) complex *cis/trans*-[$PtCl_2$(N≡$CCH_2C_6H_4$(*p*-CH_3))$_2$] 1d and its reactions with 1,3-diiminoisoindoline 2

Reaction of platinum(II) chloride with p-tolylacetonitrile

Platinum(II) chloride (200 mg, 0.752 mmol) was added at room temperature to *p*-tolylacetonitrile (5 mL), and the mixture was heated at 70 °C for 8 h. During the course of the reaction the green gray $PtCl_2$ powder was dissolved forming a homogeneous light yellow solution which indicated the formation of

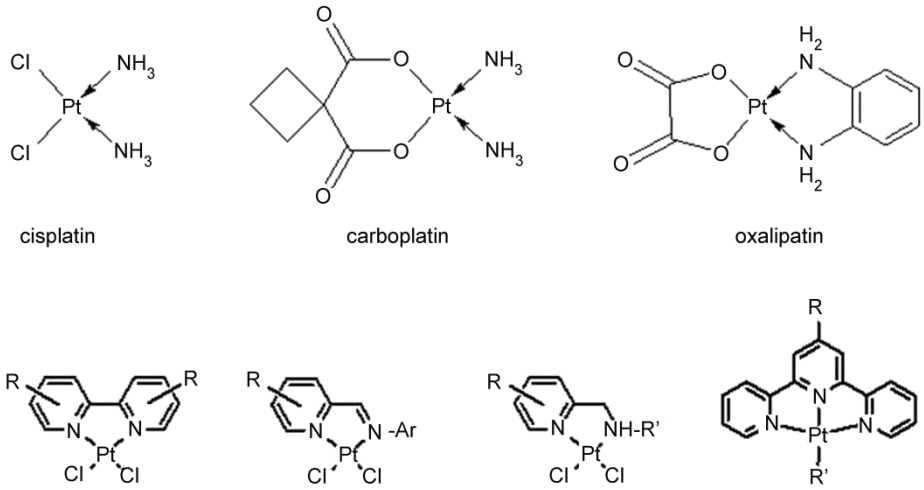

Fig. 1 — Clinically approved platinum drugs and different classes of potential anticancer pyridyl-containing platinum complexes

cis/trans-[$PtCl_2(N{\equiv}CCH_2C_6H_4(p\text{-}CH_3))_2$] **1d** complex. The obtained solution was used for the next step without further purification.

Reaction of the nitrile platinum(II) complex cis/trans-[$PtCl_2(N{\equiv}CCH_2C_6H_4(p\text{-}CH_3))_2$] 1d with 1,3-diiminoisoindoline 2

A solution of **1d** (0.532 mmol) in *p*-tolyl-acetonitrile/chloroform (10 mL, *v/v*) was added at room temperature to 1,3-diiminoisoindoline **2** (77.2 mg, 0.532 mmol), and the mixture was refluxed for 2 h whereupon the solvent was removed *in vacuo*. The crude residue was purified by column chromatography on silica (chloroform as the eluent), followed by evaporation of the solvent *in vacuo* to give the final [PtCl{NH=C($CH_2C_6H_4(p\text{-}CH_3)$)N=C($C_6H_4$)NC=NC($CH_2C_6H_4(p\text{-}CH_3)$)=NH}] **3d** product. Yield: 77%. IR (cm^{-1}): 3440 (NH), 1621 (C=N). ^{1}H NMR, δ (ppm): 2.35 (s, 6H, C*H*$_3$), 4.01 (s, 4H, C*H*$_2$), 7.20 (d, 4H, J_{HH} 7.6 Hz, $CH_{aromatic}$), 7.23 (d, 4H, J_{HH} 8.5 Hz, $CH_{aromatic}$), 7.73 (bs, 2H, $CH_{aromatic}$), 8.22 (bs, 2H, $CH_{aromatic}$), 9.69 (s, br, 2H, NH). ^{13}C NMR, δ (ppm): 21.2 (CH_3), 47.4 (CH_2), 123.3, 127.8, 127.9, 129.6, 129.8, 130.0, 130.2, 132.1 ($CH_{aromatic}$), 137.6, 137.8, 137.9, 138.8 ($C_{aromatic}$), 153.3 and 161.6 (C=N). DEPT-135 NMR, δ (ppm): 21.2 (CH_3), 47.4 (CH_2), 123.3, 127.8, 127.9, 129.6, 129.8, 130.0, 130.2, 132.1 ($CH_{aromatic}$). Anal. Calcd for $C_{26}H_{24}ClN_5Pt$ (636.137): C, 49.02; H, 3.80; N, 10.99. Found: C, 49.38; H, 3.55; N, 11.21. ESI$^+$-MS: *m/z* 635.444 $[M\text{-}1]^+$.

Computational methods

The DFT calculations were performed by Becke's three-parameter exchange functional with Lee-Yang-Parr (LYP) correlation functional. Gaussian 09 software[15] were used to performed full geometry optimizations of the compound **3d** at the B3LYP level of theory using an LANL2DZ for platinum atom and 6-311G* basis set on all other atoms. The optimization confirmed with absence of negative frequency. The Gauge-Independent Atomic Orbital (GIAO) method was used at the B3LYP /LANL2DZ/6-311G* level of theory to calculate the NMR chemical shifts with Polarizable Continuum Model (PCM). Single point TD-DFT computations were performed in order to obtain the vertical electronic transition energies. The softwares Chemcraft[16] and Multiwfn[17] were used for the analysis of Gaussian 09 output files.

Antimicrobial activity

The antibacterial activities of the tested compounds **3a-d** against *Enterococcus feacalis*, *Staphylococcus aureus* (MRSA), *Pseudomonas aeruginosa*, *Salmonella enterica*, *Escherichia coli* and *Klebsiella pneumonia* were determined using paper disc diffusion method. These bacteria were obtained from King Faisal Hospital and Research Center, Jeddah, Saudi Arabia on blood agar and preserved on nutrient agar slants at 4 °C until used. A paper disk, 7 mm diameter, loaded with the tested material (15 µg/disc) was put on Mueller Hinton agar (Sigma-Aldrich) plate, inoculated with the tested bacterium (100 µL of 4×10^6 CFU/mL). After incubation at 37 °C for 2 days, mean inhibition zone diameter of three reading was calculated in mm[18]. The antifungal activity against two species of *Candida* was detected on PDA medium and the incubation was carried out at 37 °C for 4 days. The minimum inhibitory concentrations (MICs) were determined using broth microdilution method[19].

Cell toxicity using Artemiasalina as a test organism

Artemia-based toxicity assay are cheap, continuously available, simple and reliable, and are thus an important routine work of toxicity screening. Brine shrimp lethality test was used to determine cell toxicity of the tested materials **3a-d** using *Artemiasalina* as a test organism[20]. After egg hatching, larvae were collecting and certain numbers were treated with different concentrations of the tested materials. After 8 h, surviving or dead larvae percentages were determined and lethal dose (LD50) was calculated[21,22].

Antitumor activity

Two cell lines, human colon cancer HCT116 and human breast cancer MCF-7 were cultured in McCoy's 5a and DMEM medium, respectively, supplemented with 10% (*v/v*) FBS and 100 U/mL of penicillin, 100 µg/mL streptomycin at 37 °C in CO_2 incubator. Cells were incubated with various compounds for the indicated periods of time and cytotoxicity was determined by means of the colorimetric assay MTT (3-[4,5-dimethylthiazol-2-yl]-2,5-diphenyltetrazolium bromide)[23].

Statistical analyses

The data were expressed as means plus standard deviation and one-way ANOVA was used for statistical analysis to compare the results. Tukey test (t- test) was considered significant at $p \leq 5\%$.

DNA binding studies

The stock solution of ct-DNA was prepared in distilled water and its concentration was identified

from the UV-visible absorbance values at 260 nm using the reported ε value of 6600 M^{-1} cm^{-1}, while ratio of absorbance at 260 to that at 280 nm is 1.8 (to ensure DNA is free from protein impurities)[24]. The concentration of the obtained ct-DNA is calculated to be around 5700 μM when 1 mg was dissolved in 1 mL of water. Evaluation of the binding constants between the platinum(II) complexes **3a-d** and ct-DNA were achieved by the gradual increase in the ct-DNA concentration to a solution of the complexes (100 mM) while maintaining the pH at 7.4, and using a buffer system (5 mM Tris-HCl/50 mM NaCl). The titration process was followed by the spectroscopic responses in absorption spectroscopy at 270 nm[25]. The binding constants (K_b) were calculated from the plotting of $A_o/(A - A_o)$ against 1/[DNA] in accordance to Benesi-Hildebrand equation:

$$\frac{A_0}{A - A_0} = \frac{\varepsilon_G}{\varepsilon_{H-G} - \varepsilon_G} + \frac{\varepsilon_G}{\varepsilon_{H-G} - \varepsilon_G} \times \frac{1}{K_b[DNA]} \quad \ldots (1)$$

$A_o/(A - A_o)$ is plotted against 1/[DNA] and K_b values were calculated from the ratio of the intercept to slope[26], where A_o and A are the absorbance values of the compounds in the absence and presence of ct-DNA, respectively[27].

In order to determine the binding mode of complexes **3a-d**, changes in viscosity were measured by keeping the ct-DNA concentration constant and varying the concentration of platinum(II) complexes. Viscosity experiments were carried out using Calibrated-Cannon-Fenske Routine viscometer universal size 450 at 25 °C. Flow time was measured for each sample three times, and an average flow time was calculated. The data were plotted as $(\eta/\eta_0)^{1/3}$ versus [complex]/ [DNA] ratio, where η and η_0 are the relative viscosity of DNA in the presence and absence of entitled complexes, respectively[28].

Molecular docking studies

Molecular docking studies were conducted by Molecular Operating Environment (MOE) 2008.10 (Moe source: Chemical Computing Group Inc., Quebec, Canada, 2008), a Gaussian contact surface around the binding sites were drawn, then the surface enclosed the van der Waals surface. Finally, docking studies were done to assess the binding free energy of the complexes inside the DNA. The docking scores were initially obtained utilizing London dG scoring function in MOE software and were upgraded using two unrelated refinement methods. The Grid-Min pose and the force-filed were employed to check that the refined poses of the complexes meet the correct geometrical conformations. Bonds' rotations were allowed and the best five binding poses were directed for analysis. The docking poses of the platinum(II) complexes **3a-d** and the co-crystallized structure of the ct-DNA were docked together and RMSD values were used to evaluate the best binding pose.

Results and Discussion

Reactions of bis(nitrile)platinum(II) complexes 1 with 1,3-diiminoisoindoline 2

In a previous work, several methodologies were used to synthesise metal-complexes containing C–N and/or C–O bonds *via* addition of nucleophiles[29] or 1,3-dipoles[30] to metal-activated organonitriles. Recently, we have reported that 1,3-diiminoisoindoline displays good nucleophilic properties toward additions to various bis(nitrile) platinum(II) complexes *cis/trans*-[$PtCl_2(N{\equiv}CR)_2$][14]. The 1,3-diiminoisoindoline contains two *sp²-N* nucleophiles and one endocyclic *sp³-N* moiety which can be deprotonated and then coordinated to platinum(II) centre. In addition, the nucleophilic additions of imino groups to both nitrile ligands furnishes (1,3,5,7,9-pentaazanona-1,3,6,8-tetraenato)platinum(II) compounds (Fig. 2).

The platinum(II)-bound nitriles *cis/trans*-[$PtCl_2(N{\equiv}CR)_2$]**1** (R = CH_3 (**1a**), C_2H_5 (**1b**), C_6H_5 (**1c**), $CH_2C_6H_4$(*p*-CH_3) (**1d**)) were synthesised, in excellent yields (*ca.* 90%), by reaction of platinum(II) chloride with the respective nitriles. Treatment of **1a-d** with 1,3-diiminoisoindoline HN=CC_6H_4C(NH)= NH **2**, in refluxing chloroform for 2 h, affords symmetrical (1,3,5,7,9-pentaazanona-1,3,6,8-tetraenato) platinum (II) compounds [PtCl{NH=C(R)N=C(C_6H_4) NC=NC (R)=NH}] **3a-d** in good yields (65–77%) (Scheme 1).

The IR spectrum of **3d** does not show υ(N≡C) values (2250-2350 cm^{-1} range), while new bands due to υ(NH) and υ(N=C) are observed at 3440 and 1621cm^{-1}, respectively. In the ^{1}H NMR spectrum of **3d**, the signal of the two methyl groups (CH_3) appears

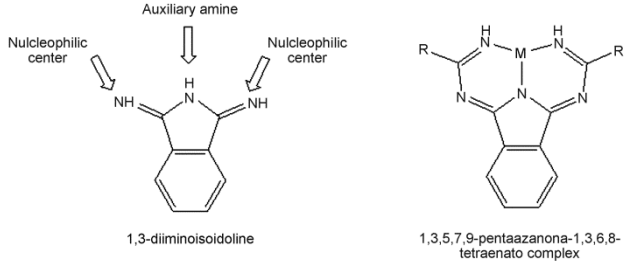

Fig. 2 — 1,3-Diiminoisoindoline and 1,3,5,7,9-pentaazanona-1,3,6,8-tetraenato complex

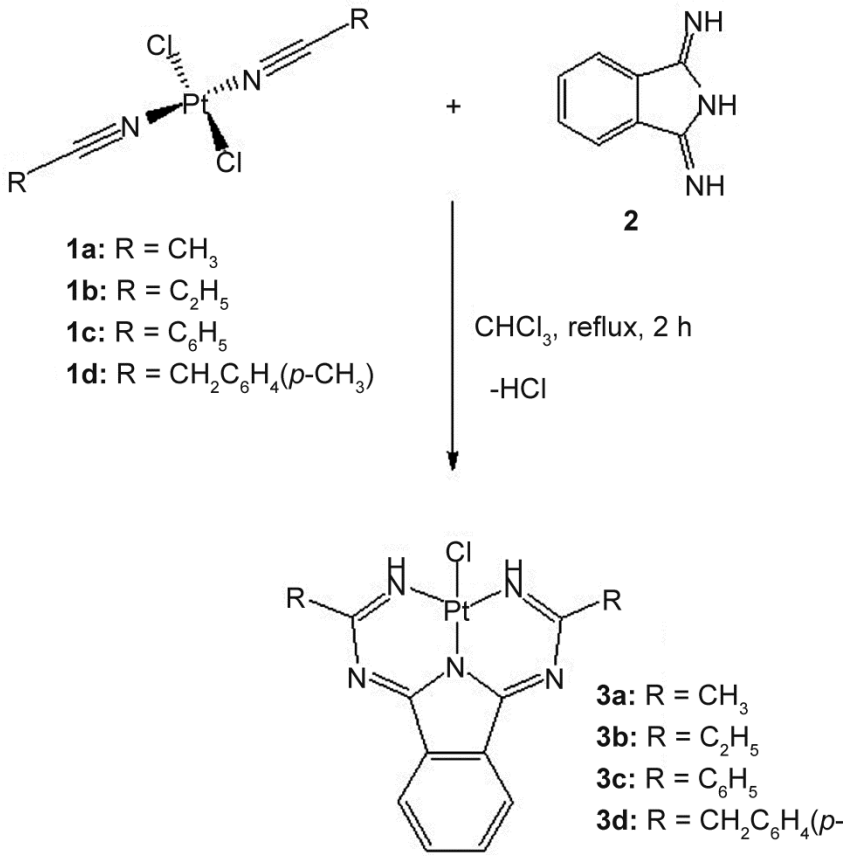

Scheme 1 — Synthesis of symmetrical (1,3,5,7,9-pentaazanona-1,3,6,8-tetraenato)platinum(II) complexes **3a-d**

as a singlet at δ 2.35; the signals of the four aromatic protons of the isoindole moiety appear as two broad signals at δ 7.73 and 8.22, respectively; and the two NH protons are exhibited at δ 9.69. The ^{13}C NMR spectrum of **3d** shows the characteristic signals of the imine N=C groups at δ 153.3 and 161.6, and the absence of the nitrile N≡*C* resonance at 118 ppm confirms that the addition of 1,3-diiminoisoindoline **2** occurs to both *p*-tolylacetonitrile ligands in **1d** (see Supplementary Data, Fig. S1).

Computational study

Geometry optimization

The structure of the complex **3d** was optimized using DFT at the B3LYP/LANL2DZ/6-311G* level of theory (Fig. 3). Selected bond lengths, bond and torsion angles are shown in Table 1. These data are in agreement with the experimental of similar complexes[14]. The square-planar coordination environment of the platinum(II) centre is defined by the monoanionic tridentate N^N^N ligand and one chloride anion, comprising two fused six-membered metallacycles defined by [N^C^N^C^N^Pt] atoms.

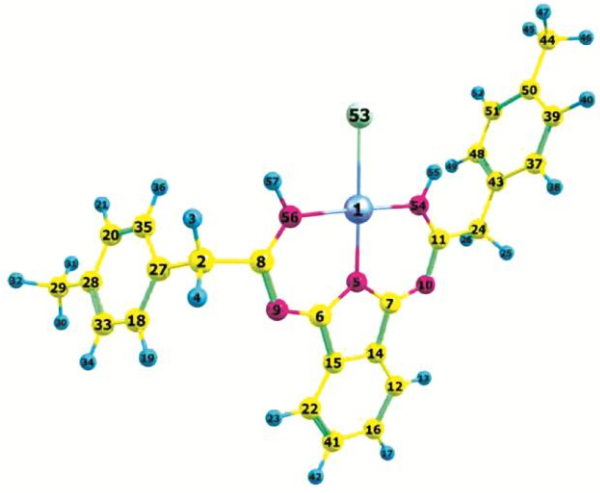

Fig. 3 — Optimized structure of complex **3d**

NMR analysis

The ^{1}H and ^{13}C NMR spectra of the platinum(II) complex **3d** were recorded experimentally in deuterated chloroform and they were calculated using B3LYP/LANL2DZ/6-311G* level of theory with GIAO approach in chloroform. The chemical shifts

Table 1 — Selected geometric parameters (Å, °) of complex **3d** compared to reference[14]

Pt1-Cl53	2.411 [2.3178(16)[a], 2.3250(17)[b]]	Pt1-N56	2.000 [1.972(5)[a], 1.972(5)[b]]
Pt1-N54	2.002 [1.972(5)[a], 1.974(5)[b]]	Pt1-N5	1.983 [1.961(6)[a], 1.942(5)[b]]
Cl53-Pt1-N54	91.40 [90.66(11)[a], 91.67(17)[b]]	N54-Pt1-N56	177.69 [178.7(2)[a], 178.5(2)[b]]
Cl53-Pt1-N56	90.91 [90.66(11[a]), 89.73(17)[b]]	N5-Pt1-N56	88.86 [89.34(11)[a], 88.9(2)[b]]
Cl53-Pt1-N5	179.53 [180.0[a], 178.28(16)[b]]	N5-Pt1-N54	88.83[89.34(11)[a], 89.7(2)[b]]

[a] reference[14a]; [b] reference[14b]

Table 2 — Comparison of the calculated chemical shifts (GIAO B3LYP/6-311G*) with the experimental (in $CDCl_3$) for complex **3d**

H			C-13		
Atom	Exp	DFT	Atom	Exp	DFT
H-13,H-23	8.22	8.30	C-11	161.60	171.11
H-57	9.69	8.23	C-8	161.60	169.76
H-42, H-17	7.73	7.88	C-6	153.31	159.63
H-19	7.24	7.77	C-7	153.31	158.72
H-40	7.23	7.58	C-50	138.81	143.48
H-55	9.69	7.42	C-28, C-15	137.88	141.72
H-52, H-49, H-38, H-36, H-34	7.20	7.42	C-14	137.88	141.61
H-21	7.19	7.30	C-27	137.85	137.79
H-25, H-26	4.01	4.47	C-41, C-16	132.13	134.20
H-4	4.01	4.28	C-43	137.60	133.70
H-3	4.01	4.01	C-48	132.12	133.33
H-47	2.35	2.78	C-37	130.21	133.15
H-46, H-32	2.35	2.60	C-18	129.99	132.64
H-31	2.35	2.30	C-39	129.78	132.36
H-30, H-45	2.35	2.19	C-51	129.63	132.03
			C-20	127.95	131.18
			C-33, C-35	127.81	130.93
			C-22	123.30	125.30
			C-12	123.30	125.18
			C-2	47.40	50.17
			C-24	47.40	48.16
			C-44	21.20	19.77
			C-29	21.20	19.55

for ^{1}H and ^{13}C nuclei in solution and theoretical values are shown in Table 2. The chemical shifts in the ^{1}H and ^{13}C NMR spectra were assigned with the help of DFT calculations of shielding constants. The theoretically calculated chemical shifts were in good agreement with the experimental ones, and the correlation coefficients for ^{1}H were 0.9947 (Fig. 4a) with excluding the imine protons because they are showing deviations from trend (labile protons), since protons attached to nitrogen are solvent and environment dependent, it is not easy to compare their theoretical values with the experimental ones[31]. The correlation coefficients for ^{13}C were 0.9968 (Fig. 4b).

Molecular orbital analysis

Frontier molecular orbitals (FMOs) play crucial role in the chemical stability, optical properties and biological activities of the molecules and also in the interactions between atoms. Among these, the highest occupied molecular orbital (HOMO) and the lowest unoccupied molecular orbital (LUMO) are the most important. Fig. 5, showed the electron density of the HOMO–2, HOMO–1, HOMO, LUMO, LUMO+1, and LUMO+2 molecular orbitals. Analysis of these orbitals showed that these orbitals are mainly composed of combination of atomic orbitals of the Pt, C, N and Cl atoms. The composition of each orbitals are shown in Table 3.

HOMO and LUMO analysis showed that composition of HOMO is mainly consisting of 21.55% dxy of Pt, 5.64% dxz of Pt, and 42.36% Pz of Cl ions. While, the LUMO is mainly consisting of 5.90% dxz of Pt, 13.16% Pz of C6, 12.70% Pz of C7, 5.86% Pz of C8, 8.28% Pz of N9, 9.00% Pz of N10, 11.38% Pz of N54 and 11.91% Pz of N56.

Molecular electrostatic potential

Molecular electrostatic potential (MEP) is used to investigate the nucleophilic or electrophilic regions in a molecule. The surface of the complex **3d** was plotted over an optimized electronic structures using B3LYP/LANL2DZ/6-311G* as shown in Fig. 6. The most positive (blue) regions are localized on hydrogen atoms of phenyl rings, showing electrophilic reactivity; whereas the most negative (red) regions are observed around the chloride ion showing nucleophilic reactivity. This result suggest that the chloride ion is very important for binding of this molecule with DNA in term of nucleophilic or electrophilic attack in hydrogen-bonding interactions and for the understanding of the process of biological recognition.

Antimicrobial activity

Multidrug resistant bacteria that resist to at least two antibiotics is due to the accumulation of different resistant genes and/or increased expression of genes that code for multidrug efflux pumps leading to an increase in human death every day[32]. The antibacterial activities of compounds **3a-d** were determined against six different multidrug resistant bacterial pathogens and some pathogenic yeasts. Complexes **3a-c** showed moderate activities against all tested gram negative

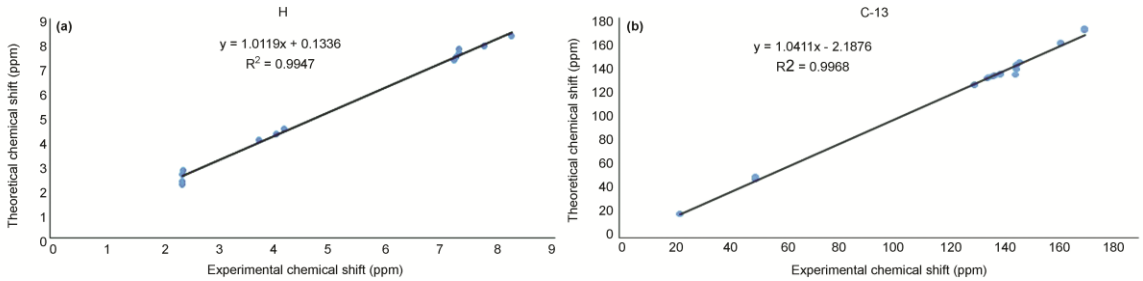

Fig. 4 — Plots of experimental *vs* calculated chemical shifts (ppm) of (a) ^{1}H and (b) ^{13}C NMR of the platinum(II) complex **3d**

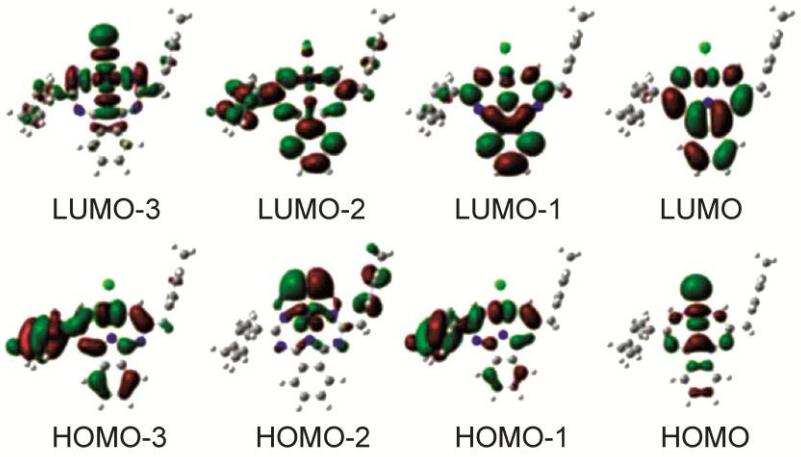

Fig. 5 — Molecular orbital shapes of platinum(II)pincer3d using B3LYP/6-311G*

Table 3 — Composition of atoms in molecular orbitals for complex **3d**

Atom	Molecular orbital composition (%)					
	HOMO-2	HOMO-1	HOMO	LUMO	LUMO+1	LUMO+2
1(Pt)	4.36	15.13	30.65	8.42	7.54	58.37
5(N)	-	2.00	9.10	-	15.71	10.39
6(C)	-	-	-	12.52	5.50	-
7(C)	-	-	-	12.03	6.14	-
8(C)	-	-	-	-	14.20	-
9(N)	-	11.82	4.27	7.88	-	-
10(N)	-	13.47	4.22	8.52	-	-
11(C)	-	-	-	-	13.82	-
12(C)	-	-	-	-	7.88	-
18 (C)	6.69	-	-	-	-	-
20(C)	8.13	-	-	-	-	-
22(C)	-	-	-	-	7.59	-
27(C)	24.23	-	-	-	-	-
28(C)	24.81	-	-	-	-	-
53(Cl)	7.20	36.98	42.73	-	-	12.01
54(N)	-	-	2.72	10.36	5.76	6.32
56(N)	-	-	2.82	10.82	5.70	6.43

bacteria while excellent activities were recorded against the three tested gram positive bacterial pathogens, *Enterococcus faecalis*, *Staphylococcus aureus* and MRSA (Table 4). The mean diameter of inhibition zones were ranged between 17-22 mm for gram positive bacteria and between 10-13 mm for gram negative ones. Very weak activity was recorded for complex **3d** compared to control antibiotic (Ampicillin). The antifungal activity against *Candida albicans* and *C. tropical* were recognized for complexes **3c** and **3d** (Table 5) with MICs ranged from 0.05 to 0.1 µM, while complexes **3a** and **3b**

showed no antifungal activities (data not shown). MIC of each compound was determined for MRSA and *E. faecalis*, the lowest MICs of **3a** and **3b** (0.03 - 0.06 µM) were recorded for the two tested bacteria, and the MIC of **3c** (0.05 µM) was recorded only for *E. faecalis* (Table 6). Similarly, the synthesized *N*-naphtylen diamine platinum(II) chloride inhibited bacterial growth and division specially *Pseudomonas aeruginosa* and *E. coli* at 15 mg/mL[33]. No toxicity was recorded against *Artemia saline* as a test organism for **3a-c**, while moderate toxicity was found for **3d** (Table 6).

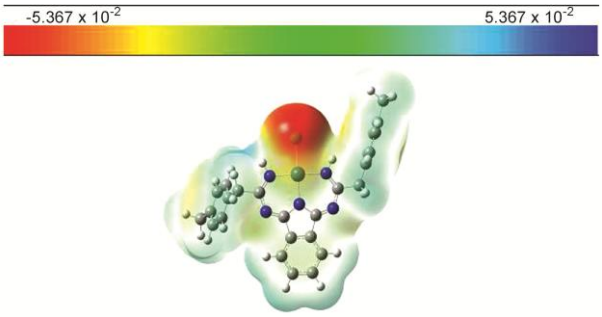

Fig. 6 — Molecular electrostatic potential map of the platinum(II) pincer **3d**

Antitumor activity

The *in vitro* cytotoxic activities of the compounds **3a-d** were recorded against human colon HCT116 and human breast (MCF-7) cancer cell lines with IC_{50} about 2.426-3.955 µM (Table 6). These results were higher than those obtained for platinum-sensitive and -resistant human ovarian cancer cell lines, as well as for colon cancer (SW948) and testicular cancer cell lines (N-TERA)[24].The study of the antitumor activities of the mixed ligand platinum(II) oxadiazoline complexes with hexamethylenetetramine and 7-nitro-1,3,5-triazaadamantane on human cancer cell lines HeLa and A549 showed that the IC_{50} was ranged from 2.5 to 10 µM and some complexes were more effective than cisplatin[34]. It is clear that cisplatin showed cytotoxicity in MCF7 cells and the calculated IC_{50} was 5.75±0.07 µM[35]. Similar to our results, platinum(II) complexes with isoniazid-derived

Table 4 — The antibacterial activities of the tested compounds **3a-d** against different human pathogens and compared to control antibiotic

Tested bacteria	Diameter of inhibition zone (mm)			
	3a	**3b**	**3c**	**3d**
Escherichia coli	13.2±0.19	11.4±0.99	11.2±0.99	7.2±1.6
Klebsiella pneumoniae	12.5±0.52	11.1±1.59	11.0±1.14	7.5±1.67
Salmonella enterica	11.2±0.22	11.1±2.03	11.7±1.09	9.2±1.26
Pseudomonas aeruginosa	10.5±0.46	11.4±1.40	10.9±1.17	10.5±0.77
Proteus mirabilis	10.5±0.43	11.3±2.00	10.5±0.43	7.5±0.45
Enterococcus faecalis	17.5±0.67	17.3±1.0 7	19.5±0.67	9.15±0.74
Staphylococcus aureus	16.5±0.64	17.2±0.19	19.2±1.14	9.12±0.14
MRSA	17.2±0.33	17.5±0.52	22.5±2.50	8.5±0.32

MRSA: Methicillin-resistant *Staphylococcus aureus*, 15mg per disc

Table 5 — Antifungal activity of complexes **3c** and **3d** compared to Amphotericin B

Tested fungi	Diameter of inhibition zone (mm)			MIC	
	3c	**3d**	Amphotericin B (Control)	**3c**	**3d**
C. albicans ATCC 90028	15.4 ±1.3	17.3 ±1.4	21. 1	0. 05*	0. 05*
C. tropicals ATCC 750	17.1±1.9	14.1 ±1.7	11.9	0.10*	0.10*

MIC of control 1-6x10^{-4} µM, * sigificant results compared to control

Table 6 — MIC, Toxicity (LD50) and antitumor activity of the tested complexes **3a-d** compared to positive control

Tested compound	MIC (µM)		Toxicity (LD_{50}, µM)	Antitumor activity (IC_{50}, µM)	
	MRSA	*E. faecalis*		Human colon HCT116	Human breast(MCF-7)
3a	0. 03*	0. 07*	>0.87	2.700	3.955*
3b	0. 06*	0. 06*	>0.82	2.426	2.426*
3c	0. 11	0. 05*	>0.68	1.889*	2.462*
3d	0. 20*	0.10*	0.62*	1.850*	2.775
Control[#]	0.14	0.02	0.88	2.970	3.331

#Control was either Ampicillin in case of bacteria, $CuSO_4$ in case of toxicity, and cisplatin in case of antitumor activity, * significant results compared to control

compound possess both antitumor and antimicrobial activities where they inhibited proliferation of human breast cancer (MCF-7 and SKBR-3), human melanoma (A375), lung adenocarcinoma cells (NCI-H1573) and their antibacterial activity were against *E. coli*, *K. pneumoniae*, *S. aureus* and *C. albicans* strains[36].

DNA binding studies

The majority of *chemotherapeutic* platinum(II) complexes establish their anticancer activity through mechanisms involving interactions with DNA[37]. Therefore, we investigated the ability of our platinum(II) complexes **3a-d** to interact with DNA. The binding constants of the complexes were obtained using their spectroscopic responses with variant concentrations of the ct-DNA. In general, the absorption spectra of **3a-d** with the increasing concentration of ct-DNA showed similar patterns (Fig. 7). All complexes **3a-d** displayed hyperchromic response at *ca.* 270 nm with no shift in **3c** and **3d** while blue shifts were noted in **3a** and **3b**. The K_b values were determined for the complexes as described in the experimental section and the data were summarized in Table 7.

The data indicates that the binding affinities of **3c** and **3b** are higher than that of **3a** and **3d**. For **3c**, this observation can be rationalized by the presence of the phenyl groups which may contribute to the binding by

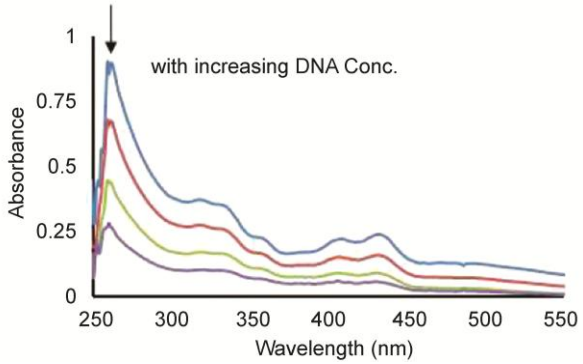

Fig. 7 — Spectral responses of **3b** while increasing the concentration of ct-DNA

Table 7 — Binding constant (K_b), spectroscopic effect at 270 nm and docking scores

Complex	Binding constant (K_b) x$10^5 M^{-1}$	Spectroscopic effect at 270 nm	Docking scores
3a	6.67 (±0.07)	Blue shift	– 4.33
3b	8.00 (±0.03)	Blue shift	– 4.27
3c	8.33 (±0.06)	No shift	– 5.27
3d	6.00 (±0.09)	No shift	– 4.20

their pi-involved interactions. Intercalation binding mode is suggested for our complexes based on the changes of absorbance, as well as the values of binding constants (K_b) of platinum(II) complexes and ct-DNA[38]. To confirm the mode of interaction, changes in the viscosity can be used as a good indication. Generally, a classical intercalative DNA binding causes an increase in DNA viscosity due to the lengthening of DNA helix, which is caused by an increase in the separation of base pairs at interaction sites and an increase in overall double helix length[39]. The relative viscosity of DNA in Tris-HCl buffer was determined by adding an increasing concentration of the complexes **3a-d** from (0-200 μM), while the ct-DNA concentration (200 μM) was kept constant. The effect of increasing the concentration of platinum(II) complexes on the viscosity of DNA at 25 °C is illustrated in Supplementary Data, Fig. S2. The results confirmed that the intercalative mode of binding exists between all platinum(II) complexes **3a-d** and ct-DNA.

Molecular docking with DNA

The molecular docking scores (Table 7) suggested that **3c** have the best score which is in agreement with the experimental binding constants. Platinum(II) complexes **3a-d** contain isoindole fragment which is believed to be interacting with DNA and the side-chains seem to influence the isoindole interaction by their steric bulkiness and/or electronic nature. According to the docking results, all complexes show an intercalation mode of binding *via* the isoindole fragment (Fig. 8). However, complexes **3c** and **3b** established pi-pi stacking with both DNA strand (A and B) while **3a** and **3d** complexes establish their stacking only with one strand of DNA(A) (Fig. 8 and Table 8). Finally for the purpose of comparison, the different biological properties were scaled by dividing

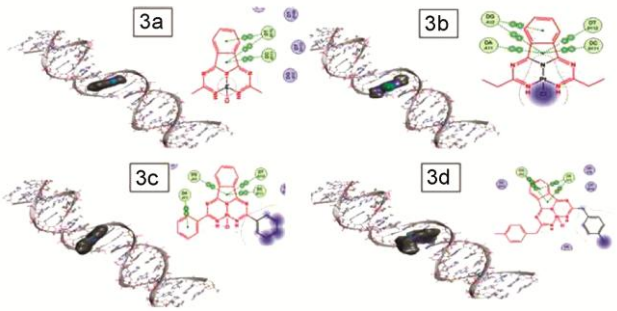

Fig. 8 — 2D and 3D views of the interactions between platinum(II) complexes **3a-d** and DNA as obtained from the docking studies

Table 8 — Different interactions of the platinum(II) complexes **3a-d** with ct-DNA in accordance to the molecular docking study

Complex	Fragment involved from the complex	Receptor in the DNA	Mode of interaction	Distance (Å)	E (kcal/mol)
3a	5-ring isoindole	6-ring DC111 (B)	pi-pi	2.83	-0.0
	5-ring isoindole	6-ring DT112 (B)	pi-pi	3.63	-0.0
	5-ring isoindole	6-ring DC111 (B)	Pi-pi	3.05	-0.0
3b	5-ring isoindole	6-ring DA11 (A)	pi-pi	3.13	-0.0
	5-ring isoindole	6-ring DG12 (A)	pi-pi	3.01	-0.0
	6-ring isoindole	6-ring DG12 (A)	pi-pi	3.24	-0.0
	5-ring isoindole	6-ring DC111 (B)	pi-pi	3.69	-0.0
	5-ring isoindole	6-ring DT110 (B)	pi-pi	3.64	-0.0
3c	5-ring isoindole	6-ring DG12 (A)	pi-pi	3.80	-0.0
	6-ring side chain	6-ring DA13 (A)	pi-pi	3.74	-0.0
	6-ring side chain	6-ring DA13 (A)	pi-pi	3.28	-0.0
	5-ring isoindole	5-ring DC11 (A)	pi-pi	2.52	-0.0
	5-ring isoindole	5-ring DT12 (A)	pi-pi	3.93	-0.0
3d	5-ring isoindole	6-ring DT12 (A)	pi-pi	3.00	-0.0
	5-ring isoindole	6-ring DT12 (A)	pi-pi	3.77	-0.0
	6-ring isoindole	5-ring DT12 (A)	pi-pi	3.45	-0.0

Only pi-pi interactions of distances higher than or equal 2.5 Å were listed (shortest pi-pi reported experimentally[40])

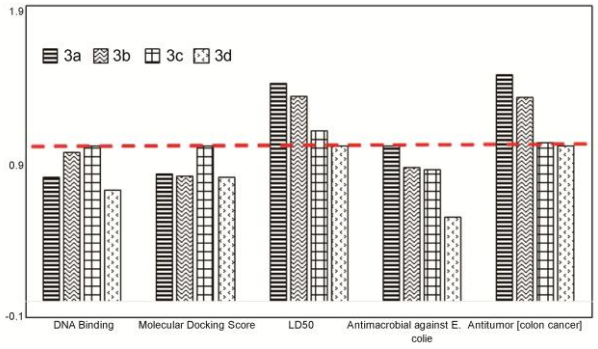

Fig. 9 — Comparison of the biological properties (scaled values) for complexes **3a-d**

all the other values within a property on the best value; hence the best complex would have a scaled value equal to one. All the different scaled properties for all complexes are plotted in Fig. 9. It is clear that complex **3c** has in total the best biological activities.

Conclusions

The reaction between *cis/trans*-[$PtCl_2(N{\equiv}CR)_2$] **1** and 1,3-diiminoisoindoline **2** afforded symmetrical (1,3,5,7,9-pentaazanona-1,3,6,8-tetraenato) Pt(II) complexes **3a-d** in a base-free protocol in contrast to their nickel(II) analogues. Complex **3d** was optimized using DFT at the B3LYP/LANL2DZ/6-311G* level of theory and its electronics structure was described in terms of the distribution of the HOMO and LUMO. GIAO method was used to calculate the NMR spectra, the correlations between the calculated and experimental chemical shifts are 0.9947 for ^{1}H and 0.9968 for ^{13}C. MEP shows that the most positive (blue) regions are localized on the hydrogen atoms of the phenyl groups showing electrophilic reactivity; whereas the most negative (red) regions are observed around the chloride atom. The antimicrobial studies revealed that the platinum(II) complexes **3a-d** showed good activities against gram positive bacteria and moderate activities against gram negative bacteria. The anticancer studies of these complexes against the two cisplatin-resistant cell lines showed their potential as anticancer drugs. The DNA-binding studies and the molecular docking indicated a strong binding of the complexes toward ct-DNA through intercalation mode of bonding by their isoindole unit. Among the studied complexes, complex **3c** has IC_{50}, binding constant to ct-DNA and docking score values better than complexes (**3a**, **3b**, **3d**) which may result from the presence of the phenyl rings in the side chains on the ligand. The notable variations in the IC_{50} values, binding constants and molecular docking scores indicate the significance of the side-chains on the ligands in tuning these properties. Moreover, the side-chains can be used to modify some chemical and physical properties of this class of platinum(II) complexes which can help in some other aspects such as the solubility and cell membrane transmittance.

Supplementary Data

Supplementary data associated with this article are available in the electronic form at http://nopr.niscair.res.in/jinfo/ijca/IJCA_60A(04)519-530_SupplData.pdf.

References

1 Petruzzella E, Sirota R, Solazzo I, Gandin V & Gibson D, *Chem Sci*, 9 (2018) 4299.

2 Butler J S & Sadler P J, *Curr Opin Chem Biol*, 17 (2013) 175.

3 Vo V, Kabuloglu-Karayusuf Z G, Carper S W, Bennett B L & Evilia C, *Bioorg Med Chem*, 18 (2010) 1163.

4 Bal S & Bal S S, *Monatsh Chem*, 146 (2015) 903.

5 Wang X & Guo Z, *Chem Soc Rev*, 42 (2013) 202.

6 (a) Buffin B P, Fonger E B & Kundu A, *Inorg Chim Acta*, 355 (2003) 340; (b) Li L J, Yan Q Q, Liu G J, Yuan Z, Lv Z H, Fu B, Han Y J & Du J L, *Biosci Biotechnol Biochem*, 81 (2017) 1081.

7 Motswainyana W M, Onani M O, Mediehe A M, Saibu M, Jacobs J & van Meervelt L, *Inorg Chim Acta*, 400 (2013) 197.

8 (a) Zeglis B M, Pierre V C & Barton J K, *Chem Comm*, (2007) 4565; (b) Fisher D M, Fenton R R& Aldrich-Wright J R, *Chem Comm*, (2008) 5613.

9 Bond P J, Langridge R, Jennette K W & Lippard S J, *Proc Natl Acad Sci USA*, 72 (1975) 4825.

10 (a) Bugarčić Z D, Heinemann F W & van Eldik R, *Dalton Trans*, (2004) 279; (b) Petrović D, Stojimirović B, Petrović B, Bugarčić Z M & Bugarčić Z D, *Bioorg Med Chem*, 15 (2007) 4203.

11 McFadyen W D, Wakelin L P, Roos I A & Leopold V A, *J Med Chem*, 28 (1985) 1113.

12 (a) Todd J A, Turner P, Ziolkowski E J &Rendina L M, *InorgChem*, 44 (2005) 6401; (b) Woodhouse S L, Ziolkowski E J &Rendina L M, *Dalton Trans*, (2005) 2827.

13 Ma D-L, Shum T Y-T, Zhang F, Che C-M & Yang M, *Chem Comm*, (2005) 4675.

14 (a) Lasri J, Pedras B, Haukka M & Berberan-Santos M N, *Polyhedron*, 133 (2017) 195; (b) Lasri J, Kuznetsov M L, Guedes da Silva M F C & Pombeiro A J L, *Inorg Chem*, 51 (2012) 10774.

15 Frisch M J, Trucks G W, Schlegel H B, Scuseria G E, Robb M A, Cheeseman J R, Scalmani G, Barone V, Mennucci B, Petersson G A, Nakatsuji H, Caricato M, Li X, Hratchian H P, Izmaylov A F, Bloino J, Zheng G, Sonnenberg J L, Hada M, Ehara M, Toyota K, Fukuda R, Hasegawa J, Ishida M, Nakajima T, Honda Y, Kitao O, Nakai H, Vreven T, Montgomery Jr J A, Peralta J E, Ogliaro F, Bearpark M, Heyd J J, Brothers E, Kudin K N,Staroverov V N, Kobayashi R, Normand J, Raghavachari K, Rendell A, Burant J C, Iyengar S S, Tomasi J, Cossi M, Rega N, Millam J M, Klene M, Knox J E, Cross J B, Bakken V, Adamo C, Jaramillo J, Gomperts R, Stratmann R E, Yazyev O, Austin A J, Cammi R, Pomelli C, Ochterski J W, Martin R L, Morokuma K, Zakrzewski V G, Voth G A, Salvador P, Dannenberg J J, Dapprich S, Daniels A D, Farkas O, Foresman J B, Ortiz J V, Cioslowski J & Fox D J, *Gaussian 09, Revision A02, Gaussian Inc, Wallingford CT, USA*, 2009.

16 Chemcraft software, http://www.chemcraftprog.com, 2019.

17 (a) Lu T & Chen F, *J Comput Chem*, 33 (2012) 580; (b) Lu T & Chen F, *Acta Chim Sinica*, 69 (2011) 2393.

18 Westley J, Evans Jr R H , Sello L H & Troupe N, *J Antibiot*, 32 (1979) 100.

19 Hudzicki J, *Kirby-Bauer disk diffusion susceptibility test protocol*, American Society for Microbiology, Washington DC, 2009.

20 Sangian H, Faramarzi H, Yazdinezhad A, Mousavi S J, Zamani Z & Noubarani M, *Parasitol Res*, 112 (2013) 3697.

21 Meyer B N, Ferrigni N R, Putnam J E, Jacobsen L B, Nichols D E & McLaughlin J L, *Planta Med*, 45 (1982) 31.

22 Aly M M & Gumgumjee N M, *Afr J Biotechnol*, 10 (2011) 12058.

23 Coley H M, Sarju J & Wagner G, *J Med Chem*, 51 (2008) 135.

24 Kennard O, *Pure Appl Chem*, 65 (1993) 1213.

25 Marmur J, *J Mol Biol*, 3 (1961) 208.

26 Hosny N M, Hussien M A, Radwan F M & Nawar N, *Spectrochim Acta Part A*, 132 (2014) 121.

27 Eweas A F, Khalifa N M, Ismail N S, Al-Omar M A & Soliman A M, *Med Chem Res*, 23 (2014) 76.

28 Saeidifar M, Mirzaei H, Nasab N A &Mansouri-Torshizi H, *J Mol Struct*, 1148 (2017) 339.

29 (a) Kopylovich M N, Karabach Y Yu, Guedes da Silva M F C, Figiel P J, Lasri J & Pombeiro A J L, *Chem Eur J*, 18 (2012) 899; (b) Kopylovich M N, Lasri J, Guedes da Silva M F C & Pombeiro A J L, *Eur J Inorg Chem*, (2011) 377; (c) Figiel P J, Kopylovich M N, Lasri J, Guedes da Silva M F C, Fraústo da Silva J J R & Pombeiro A J L, *Chem Comm*, 46 (2010) 2766; (d) Kopylovich M N, Lasri J, Guedes da Silva M F C & Pombeiro A J L, *Dalton Trans*, (2009) 3074; (e) Lasri J, Guedes da Silva M F C, Januário Charmier M A & Pombeiro A J L, *Eur J Inorg Chem*, (2008) 3668; (f) Lasri J, Januário Charmier M A, Guedes da Silva M F C & Pombeiro A J L, *Dalton Trans*, (2007) 3259; (g) Lasri J, Januário Charmier M A, Guedes da Silva M F C & Pombeiro A J L, *Dalton Trans*, (2006) 5062.

30 (a) Lasri J, Eltayeb N E,Haukka M & Babgi B A, *Polyhedron*, 158 (2019) 65; (b) Lasri J, Soliman S M, Januário Charmier M A, Ríos-Gutiérrez M & Domingo L R, *Polyhedron*, 98 (2015) 55; (c) Lasri J, *Polyhedron*, 57 (2013) 20; (d) Lasri J, Fernández Rodríguez M J, Guedes da Silva M F C, Smoleński P, Kopylovich M N, Fraústo da Silva J J R & Pombeiro A J L, *J Organomet Chem*, 696 (2011) 3513; (e) Fernandes R R, Lasri J, Guedes da Silva M F C, Palavra A M F, da Silva J A L, Fraústo da Silva J J R & Pombeiro A J L, *Adv Synth Catal*, 353 (2011) 1153; (f) Lasri J, Guedes da Silva M F C, Kopylovich M N, Mukhopadhyay B G & Pombeiro A J L, *Eur J Inorg Chem*, 36 (2009) 5541; (g) Lasri J, Guedes da Silva M F C, Kopylovich M N, Mukhopadhyay S, Januário Charmier M A & Pombeiro A J L, *Dalton Trans*, (2009) 2210; (h) Mukhopadhyay S, Mukhopadhyay B G, Guedes da Silva M F C, Lasri J, Januário Charmier M A & Pombeiro A J L, *Inorg Chem*, 47 (2008) 11334; (i) Mukhopadhyay S, Lasri J, Guedes da Silva M F C, Januário Charmier M A & Pombeiro A J L, *Polyhedron*, 27 (2008) 2883; (j) Lasri J, Kopylovich M N, Guedes da Silva M F C, Januário Charmier M A & Pombeiro A J L, *Chem Eur J*, 14 (2008) 9312; (k) Mukhopadhyay S, Lasri J, Januário Charmier M A, Guedes da Silva M F C & Pombeiro A J L, *Dalton Trans*, (2007) 5297; (l) Lasri J, Januário Charmier M A, Haukka M & Pombeiro A J L, *J Org Chem*, 72 (2007) 750.

31 Mphahlele M J, Maluleka M M, Rhyman L, Ramasami P & Mampa R M, *Molecules*, 22 (2017) 83.

32 Haddadin A S, Fappiano S A &Lipsett P A, *Postgrad Med J*, 78 (2002) 385.

33 Chehregani A H, Sabounchi S J &Jodaian V, *Pak J Biol Sci*, 10 (2007) 641.

34 Sieste S, Lifincev I, Steina N & Wagner G, *Dalton Trans*, 46 (2017) 12226.
35 Suberu J O, Romero-Canelón I, Sullivan N, Lapkin A A & Barker G C, *Chem Med Chem*, 9 (2014) 2791.
36 Pahonțu E, Ilieș D C, Shova S, Oprean C, Păunescu V, Olaru O T, Rădulescu F Ș, Gulea A, Roșu T &Drăgănescu D, *Molecules*, 22 (2017) 650.
37 Deo K M, Ang D L, Mc Ghie B, Rajamanickam A, Dhiman A, Khoury A, Holland J, Bjelosevic A, Pages B, Gordon C & Aldrich-Wright J R, *Coord Chem Rev*, 375 (2018) 148.
38 Mashat K H, Babgi B A, Hussien M A, Arshad M N & Abdellattif M H, *Polyhedron*, 158 (2019) 164.
39 Gaber M, El-Ghamry H A, Fathalla S K & Mansour M A, *Mater Sci Eng C*, 83 (2018) 78.
40 Das P, Jain C K, Dey S K, Saha R, Chowdhury A D, Roychoudhury S, Kumar S, Majumder H K & Das S, *RSC Adv*, 4 (2014) 59344.